ACS SENSORS

pubs.acs.org/acssensors

Article

Minimalist Design for a Hand-Held SARS-Cov-2 Sensor: Peptide-Induced Covalent Assembly of Hydrogel Enabling Facile Fiber-Optic Detection of a Virus Marker Protein

Junxia Wang, Mengqi Lv, Hehuan Xia, Jialei Du,* Yiwei Zhao, Hao Li,* and Zhongyin Zhang*

Cite This: *ACS Sens.* 2021, 6, 2465−2471

Read Online

ACCESS | Metrics & More | Article Recommendations

ABSTRACT: The rampaging COVID-19 needs bioassaying methods of low cost and high robustness for those living in the poorly developed regions. Here, we propose such a method that does not need expensive and complicated equipment. Only a set of hand-held small devices is sufficient. A section along an optic fiber cable is stripped, so that laser light travelling through it will leak outside, while biosensing process taken place on this stripped section can form a new cladding layer of hydrogel, restoring the laser output of the fiber. A short peptide probe immobilized on the stripped section of the fiber can covalently capture a biomarker protein of SARS-Cov-2 from the serum sample. Through the cross-linking of the target protein with the interfering proteins in the serum sample, a hydrogel is covalently immobilized around the stripped section, highly resistant to detergent rinsing that is indispensable for removing nonspecific interference from the clinical sample. Using this "covalent biosensing" strategy, only one peptide probe is sufficient to simultaneously achieve ultrahigh affinity toward the biomarker protein of SARS-Cov-2 and effective signal amplification.

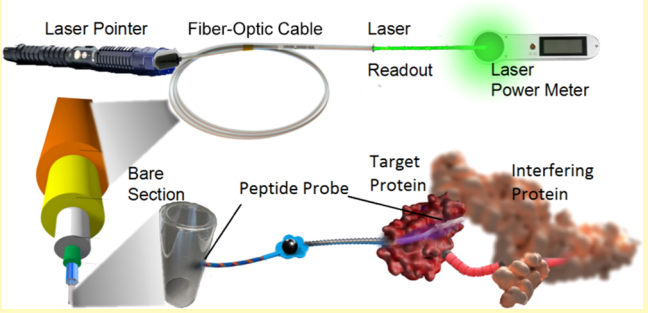

KEYWORDS: *SARS-Cov-2, peptides, covalent biosensing, fiber-optic biosensor, virus protease*

The current corona virus pandemic calls for bioassay methods of lower cost and higher robustness,[1] so that virus screening protocols can cover a larger population,[2] especially the poorer communities,[3] with more frequent sampling and greatly improved awareness of the situation.[4] A dramatic cut in the cost of bioassay can first come through replacing bio-macromolecules by artificially synthesized small molecules. For example, antibodies can be replaced by peptides[5] or aptamers[6] that can be designed and synthesized at will and are much easier to store and transport compared with the antibody. However, these synthetic probes often have reduced[7] targeting ability.[8] This can be remedied through "covalent biosensing", as we have recently demonstrated: equipping a peptide probe with a reactive "warhead", so that the peptide can place the reactive group at proper location and orientation through peptide−protein molecular recognition.[9] Then, the "warhead" can covalently and irreversibly bind with the target protein, providing ultrahigh affinity,[10] making the peptide−protein complex resistant to thorough and denaturing rinsing treatment. Moreover, such rinsing is usually indispensable for clinical applications.[11]

Here, the target protein of choice is the main protease of SARS-Cov-2.[12] This papain-like cysteine protease is a housekeeping protein essential for the replication of the virus: only after the cleavage by this enzyme, the "crude product" of genome translation matures into the replication machinery of this virus.[13] It takes only a tetrapeptide sequence to target the catalytic site of this enzyme, and successful targeting can induce covalent coupling of the catalytic cysteine of the target protein with the peptide, as demonstrated by a recent research work.[14] However, a covalent peptide probe can only deal with one half of the challenge, and the other half is how to use this peptide to generate an amplified signal, without subsequently adding any reagent into the assaying system. A commonly employed strategy is fluorescence resonance energy transfer.[15] However, this mechanism usually only works upon the dramatic change of conformation of the peptide,[16] while the tetrapeptide is not long enough to have any such conformational change. A slightly longer oligopeptide is more amiable for conformational change detection and also requires no

Received: April 27, 2021
Accepted: May 28, 2021
Published: June 9, 2021

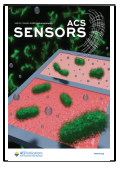

specially modified amino acid. Yet, this special tetrapeptide sequence is directly adopted from a previous report,[14] for its unique ability to covalently bind with the target protein. Moreover, no other enzymes or nanomaterials are allowed to enter the sensing system once the incubation of the peptide probes with the sample is completed. If signal amplification can still be achieved under such strict restrictions, the cost can be cut further. Perhaps a fairly large cut of cost can be expected since enzymes and nanomaterials are no longer necessary.

With no additional reagents, the only source of signal amplification is the sample itself: as we have recently demonstrated,[9] dityrosine cross-linking can be initiated under a certain circumstance, among the nonspecific interfering proteins in the clinical sample. The product of dityrosine cross-linking is a hydrogel with a distinct fluorescent signal.[17] Here, we demonstrate another way to employ this signal-amplification-through-nonspecific-protein strategy: the peptide probe is equipped with a special amino acid with a complexed ruthenium ion as the side chain.[18] Therefore, under the illumination of visible light, such as the solar radiation, tyrosine moieties of the target proteins and the nonspecific proteins alike will cross-link with each other, under the photocatalysis of the complexed ruthenium ion, as previously reported.[19] As shown in Scheme 1, in the absence of the target protein, this reaction can still proceed. However, as the peptide molecules immobilized on the sensing interface do not contain any tyrosine, the cross-linked product has no foothold on the sensing surface, so the standard clinical rinsing can remove the product from the surface. On the other hand, in the presence of the target protein, the cross-linked hydrogel can be retained on the surface by multiple covalent linkages with the target protein molecules, which are in turn covalently anchored to the surface via covalent bonding with the peptide probes. Higher target concentration means more foothold points on the surface, leading to a higher rate of retention of the hydrogel, enabling quantitative detection.

Scheme 1. Proposed Method to Detect the Main Protease of SARS-Cov-2[a]

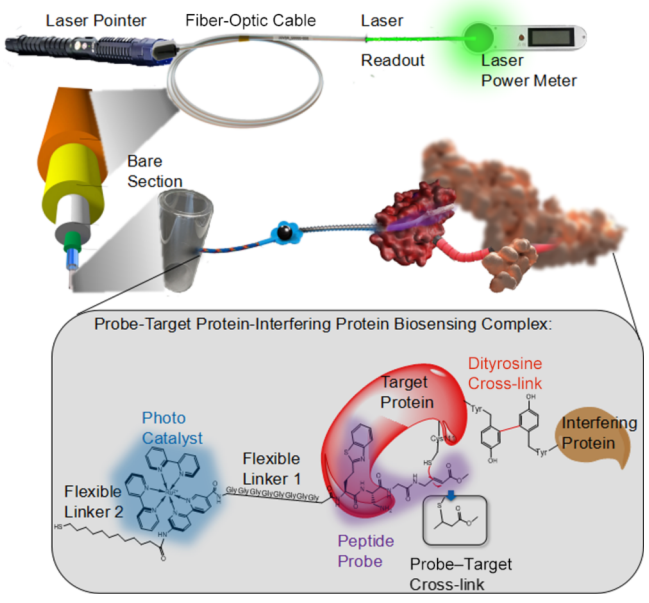

[a]Not drawn to scale.

To convert the rate of retention of the hydrogel to a signal readout, we use the hydrogel as a cladding to a laser waveguide to modulate its mode of emission.[20] This waveguide is simply formed by stripping the original cladding material off a fiber-optic cable, so that laser travelling through it will leak out of the naked cable, resulting in a very low background optical signal readout. The peptide probes are immobilized on the transparent outer surface of the naked silica core, so after dipping this naked section of the cable into the clinical sample under visible-light illumination, a new layer of hydrogel cladding can form around the cable, reducing the leakage of light and resulting in a signal-on optical read out. This simple device consists of a laser pointer, a simple mechanical coupler, a piece of fiber-optic cable with one stripped section presenting the peptide, and a hand-held power meter for collecting the read out. No fixed equipment is required.

EXPERIMENTAL SECTION

Chemicals and Reagents. Peptide probe, the sequence of which was as shown in Scheme 1, was manufactured by Jinan VR biotech, as a lyophilized powder, purity > 95%. The powder of the peptide probe was dissolved, with 10 mM phosphate-buffered saline (PBS, pH 7.4) solution, to a series of desired concentrations. The recombinant main protease of SARS-Cov-2 was purchased from Invitrogen. Analytical grade was attained for all the other reagents. The serum-spiked samples of the main protease were prepared by reconstituting the 4-(2-hydroxyethyl)-1-piperazineethanesulfonic acid solution of the recombinant protease received from the vendor with 10 mM PBS (pH 7.4), and then, the mixture was diluted to desired concentrations with the serum of a healthy volunteer. Deionized water for preparing all the solutions was produced from distilled water using a Milli-Q purification system, and a specific resistance of 18 MΩ·cm was attained, ensuring reliable purity of the dd water.

Construction of the Biosensor. To experiment with the various aspects of the proposed design, the biosensing surface was first constructed on a traditional substrate: transparent Au-sprayed indium-tin-oxide (ITO) slides (Aldrich, a layer thickness of 100 Å) were first employed as the substrate. They were cut to fit the size of the cuvettes used for fluorescence light absorbance measurement. These slides were then cleaned with a mild stream of nitrogen of high purity, while sonication in piranha solution might lead to partial or even total peeling off of the Au surface layer from the ITO substrate. Meanwhile, the transparency and the refraction index of the Au-sprayed slide were compared with those parameters of unmodified ITO glass, and it was found that the thin gold layer did not evidently alter the optic property of the ITO glass. This would provide a reference for manufacturing the optical sensor in the following. Then, the ITO slides were immersed in the "assembly solution" [2.5 μM peptide probe and 5 mM tris(2-carboxyethyl)phosphine hydrochloride (TCEP) in 10 mM PBS, pH 7.4, and TCEP was added to prevent the thiol-ended probe molecules to form a S−S bond with each other] at 4 °C and was kept under this environment for 16 h. After thorough rinsing with dd water, the slides were subsequently immersed in 9-mercaptononanol (MN) solution (1 mM MN in 10 mM PBS, pH 7.4) at room temperature for 3 h, and MN was used to occupy all the remaining active surface in between each two surface-immobilized peptide probes. The ITO slides modified in this way were subsequently used for surface plasma resonance (SPR) and electrochemical and fluorescent experiments.

The final signal readout was planned to be collected from an optical sensor built from a laser pointer and fiber-optic material. The key to achieve the desired analytical performance was to ensure that every optical element did have the expected refraction index, so that light would first leak through the exposed silica core and after cladding by the cross-linked hydrogel, light would be reflected back into the silica core to stop the leaking. First, a section (1 cm) along a piece of fiber-optic cable was stripped of its original multilayer cladding until the silica core was exposed. Specifically, the common four-core

https://doi.org/10.1021/acssensors.1c00869
ACS Sens. 2021, 6, 2465−2471

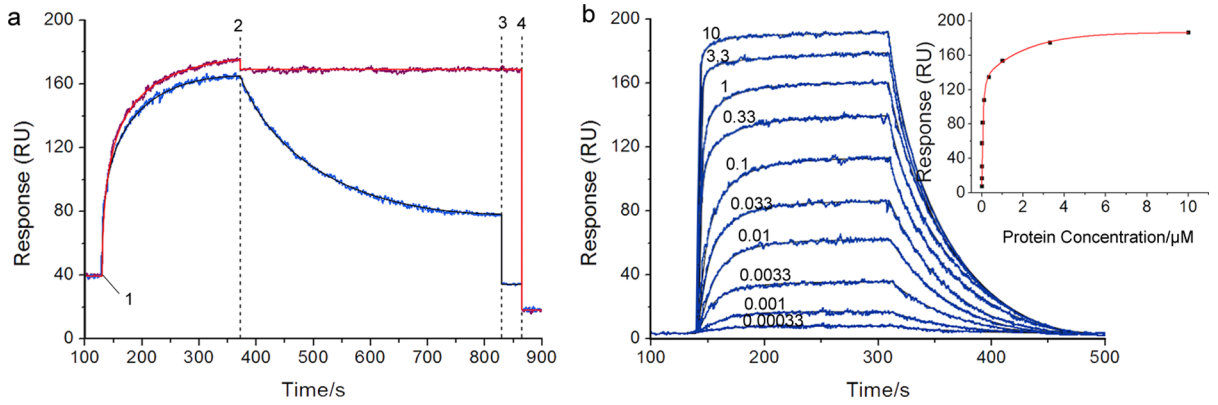

Figure 1. (a) SPR sensorgram obtained by flowing the serum-spiked recombinant protease sample (10 μM) across a sensing surface modified by the designed probe (red curve) or modified by a probe substituting the original ketoamide by a simple amide group (blue curve), so that this control probe cannot covalently bind with the target protein. The injection starts from point 1, and points 2−4 indicate the starting of the dissociation step, the addition of the detergent, and the beginning of acidic regeneration, respectively. (b) Stable flow established by titrating the sensing surface with serially diluted serum-spiked recombinant protease samples, and the inset is the relationship between the platform response and protease concentration in the diluted samples.

networking cable was stripped and one of the cores was exposed for the biosensing experiment. Strictly speaking, the "real core" of the strand where the light travels was typically around 0.5 mm. However, the cladding material immediately surrounding the "real core" was of a similar transparent glass material, and this thick layer formed a more workable "core" of 5 mm diameter. Hydrofluoric acid was then employed to erode away the glass cladding, leaving a core slightly smaller than 1 mm in diameter. The thinner core is structurally very weak without proper support. Then, the whole piece of cable was sealed inside a vacuum chamber to receive a layer of ion-sprayed Au, and the time of ion-spray was shortened to ensure that the refraction index of the Au-layered silica core was not evidently different from that of the original silica core. After Au ion-spray, the stripped section was put through the above two-step modification process.

The peptide-modified silica core was then tested for its refraction index, and the result showed a number not far away from that of the original silica core (roughly 4.5). Using both the original silica core and the peptide-modified core, it was found that around 40% light flowing through the stripped section would leak out, so the "base line" laser power readout in the power meter was around 60%. Then, an "empty" serum sample containing no main protease was incubated with the stripped section under visible-light illumination for a very long time to form a "protein membrane" of hydrogel surrounding the stripped section. Nearly 100% of all laser light flowing through the core was restored. After thorough rinsing with a detergent, this ring of hydrogel was removed from the silica core, as expected. No target protein molecules were present in this control sample to form "foothold" points on the silica core. The refraction index of the hydrogel was found to be nearly 1.5, and the index of the hydrogel formed in the presence of the target protein would be similar, as the target protein only constituted a very small fraction of all proteins in the serum-spiked sample. Therefore, the relevant physical parameters necessary for the optical sensor to work were first validated, and the sensor design would be examined and optimized in the "Results and Discussion" section.

To construct the optical sensor, a homemade mechanical coupler was employed to link up the laser pointer (power 1−5 mW, higher power and shorter wavelength might pose a real danger to eyes.) and the cable. The coupler was actually a series of clamps ensuring that the pointer and one end of the cable were co-axially aligned. The stripped section was then allowed to form a loop, facilitating incubation with the sample. The other end of the cable was brought near to the end coupled to the pointer, and a collimator lens was clamped by the coupler to improve the quality of the output laser light.

Enzyme Activity Assay. The slides or the stripped section of the fiber-optic cable were immersed in serum-spiked samples of the recombinant protease and kept at 37 °C for proper time for the surface-tethered peptide probes to noncovalently recognize their target proteins and then covalently attack them to form irreversible bonds with these target molecules. Subsequently, after thorough rinsing with sodium dodecyl sulfate detergent, the slides or the stripped section of the fiber-optic cable were ready for measurement.

Experimental Measurements. SPR measurements were conducted on an Autolab ESPRIT system (Echo Chemie B.V., Netherlands) equipped with a 670 nm monochromatic p-polarized light source. Electrochemical measurements were recorded using a CHI660D potentiostat (CH Instruments) with a routinely used "three-electrode" system: the modified ITO slide acted as the working electrode, a saturated calomel electrode (SCE) served as the reference electrode, whereas a platinum wire was used as the counter electrode. The experimental parameters for electrochemical impedance spectroscopy (EIS) are as follows: bias potential, 0.224 V vs SCE; amplitude, 5 mV; and frequency range, 0.1 Hz−10 kHz. Electrolyte solution: 5 mM $Fe(CN)_6^{3-/4-}$ with 1 M KCl. The data are obtained from at least three times of repetition of the independent experiment, and error bars are shown in the figures. Fluorescence emission spectra of the ITO surfaces were collected on a QM-4/2005 fluorescence spectrometer (Photon Technology International, Inc., Birmingham, NJ) furnished with a xenon lamp. This light source and the detector were kept in the same plane but at a right angle toward each other. The slides were put in a dd water-filled cuvette and kept at 60° from the base line of the cuvette, during the fluorescence experiments. Attention should be paid to ensure that the Au-sprayed face of the slide was in a position away from the light source and toward the detector. The peak wavelength to activate the dityrosine produced after cross-linking was 325 nm.

RESULTS AND DISCUSSION

To convert the rate of retention of the hydrogel to a signal readout, we use the hydrogel as a cladding to a laser waveguide to modulate its mode of emission.[20,21] This waveguide is simply formed by stripping the original cladding material off a fiber-optic cable, so that the laser travelling through it will leak out of the naked cable, resulting in a very low background optical signal readout. The peptide probes are immobilized on the transparent outer surface of the naked silica core, so after dipping this naked section of the cable into the clinical sample under visible-light illumination, a new layer of hydrogel cladding can be acquired by the cable, reducing the leakage of light and resulting in a signal-on optical read out. This simple device consists of a laser pointer, a simple mechanical

https://doi.org/10.1021/acssensors.1c00869
ACS Sens. 2021, 6, 2465−2471

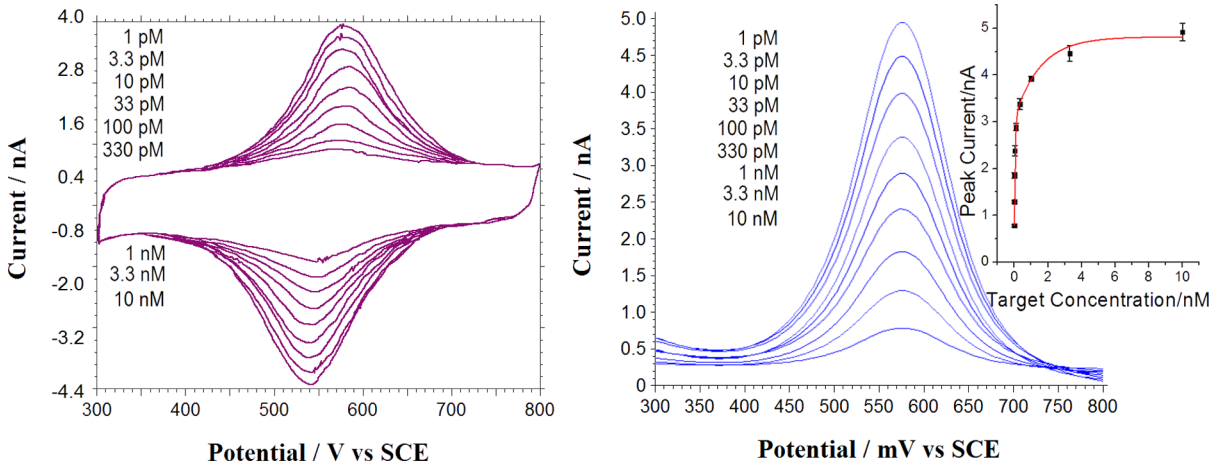

Figure 2. (a) Cyclic voltammetric peak responses obtained by incubating the sensing layer (modified on a conductive ITO slide) with serially diluted recombinant protease samples, and the estimated concentration is displayed. (b) Corresponding SWV responses. The inset is a plot showing the SWV peak responses as a function of target concentration, and error bars indicate the standard deviation (n = 3).

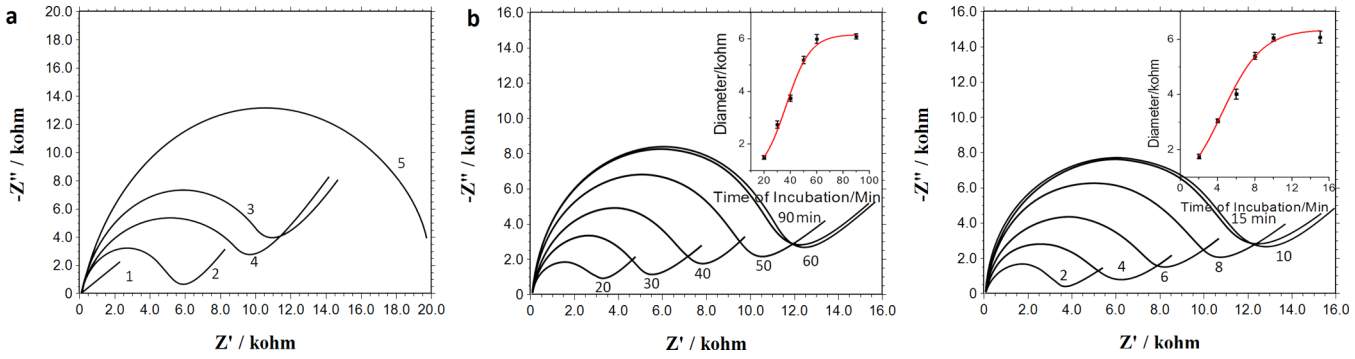

Figure 3. EIS recorded under various conditions. (a) Step-by-step characterization of the biosensing process detecting the main protease (concentration: 10 nM). (b) Time course of the interaction between the main protease (concentration: 10 nM) and a control peptide without the covalent "warhead", and the inset is the diameter of the semicircle displayed as a function of the incubation time (error bars represent the standard deviation, n = 3). (c) Similar time course recorded during the interaction with the propose peptide, and the inset is the same as the inset of (b). All the experiments are conducted in a dark room away from bright light illumination to prevent evident cross-linking between the target protein and the interfering proteins in the serum-spiked sample.

coupler, a piece of fiber-optic cable with one stripped section presenting the peptide, and a hand-held power meter for collecting the read out. No fixed equipment is required. The entire sensing system is actually composed of two small hand-held devices: the laser pointer serially connected to the cable via the coupler and the power meter. This simplicity is highly welcomed in the clinical application.

The ability of the proposed probe to recognize and then covalently bind with its designated target is studied using the SPR method. To a slide covalently modified with probe molecules, the recombinant protease sample is loaded and allowed to flow across the sensing surface. Then, the SPR readout is collected, as shown in Figure 1a. From this result, a two-step noncovalent recognition tandem covalent cross-linking can be discriminated. The noncovalent recognition is established via hydrogen bonding, so it is dynamically much faster than the covalent cross-linking, as can be seen in our result. The second step is rather slow, and from the sensorgram, it seems that a very long time is needed for the cross-linking to approach completion, so we stop the reaction when the SPR response does not increase evidently. By diluting the same batch of recombinant protease sample to different concentrations, the noncovalent binding strength of the probe exhibited during its noncovalent recognition of the target protein can be studied, as shown in Figure 1b, and the binding strength is not particularly strong, only comparable with that of the aptamer but falls very short of that of antibody.

However, because of the ability of irreversible covalent binding, the apparent binding strength should be much higher since the covalent cross-linking will pull the equilibrium toward the complex form. To verify this, an electrochemical method is enlisted. A conductive slide modified with the probe is employed as the working electrode. After covalent cross-linking with the captured targets have been accomplished, target proteins on the electrode surface are oxidized electrochemically, and peak responses can be observed on the cyclic voltammograms (Figure 2a), indicating the oxidation of tyrosine moieties of the captured target protein. Each target protein, or the main protease of COVID-19 virus, contains 11 tyrosine moieties, so the peak area from the cyclic voltammetric (CV) results can be used to calculate the number and density of surface-captured target protein molecules and those quantities of the surface-modified probe. Serially diluted recombinant protease samples are incubated with the sensing surfaces, and the resulted square wave voltammetric (SWV) responses of tyrosine oxidation are compared, as shown in Figure 2b. It can be observed that the signal response drops sharply with each dilution. From this

https://doi.org/10.1021/acssensors.1c00869
ACS Sens. 2021, 6, 2465−2471

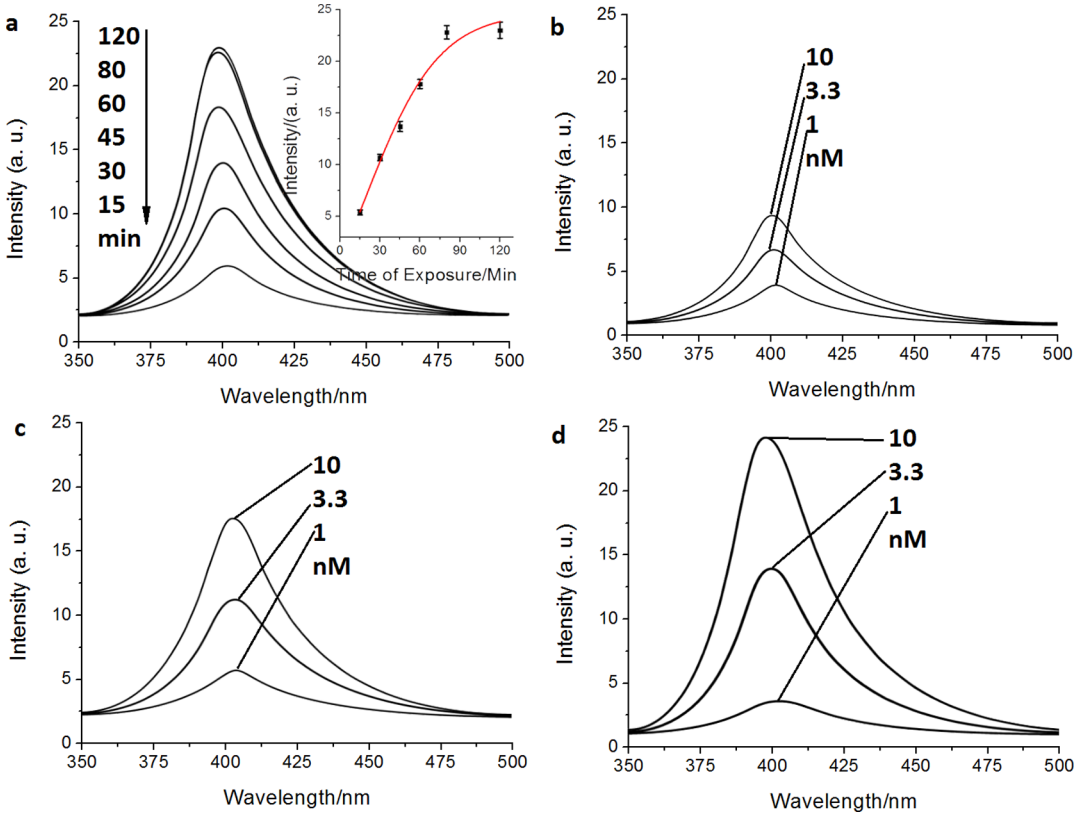

Figure 4. Fluorescent responses of dityrosine obtained under various experimental conditions. (a) Time course of the exposure to visible light recorded for incubating the blank serum sample containing no target protein with the probe-modified slide; the inset shows fluorescent peak responses as a function of exposure time, and error bars are the same as that given in Figure 3. (b–d) Fluorescent responses for detecting 10, 3.3, and 1 nM of the main protease and the responses obtained at the three concentrations after different times of exposure [10 min incubation in (b), 20 min in (c), and 30 min in (d)]; detergent rinsing is applied after light exposure.

result, it is clear that the undiluted sample contains target proteins sufficient to saturate all probe molecules on the sensing surface; this can be partly attributed to our usage of very low probe concentration when fabricating the sensing surface, so the surface density of the probe is rather low and therefore easy to be saturated by the sample with not very high concentration of the target protein.

Based on the results in Figure 2b, the CV peak response of the undiluted sample in Figure 2a can be used to calculate the number of probes on the electrode surface following the guide of Faraday's law of electrolysis. Moreover, the CV peak responses of the serially diluted samples in Figure 2a can be employed to calculate the number of target proteins covalently cross-linked on the surface. Their ratios versus the amount of the surface probe represent the constant of dissociation or the apparent binding strength. Not surprisingly, the apparent affinity after covalent cross-linking is around 30 pM (Figure 2b inset). Therefore, it can be concluded that our probe can function as a "synthetic artificial antibody", with ultrahigh strength, due to its unique ability to covalently bind with its target.

The biosensing procedure is then followed step-by-step using EIS measurements. As shown in Figure 3a, a conductive slide without probe modification appears as a straight line in the Nyquist plot (curve 1), and after the surface modification by the peptide probe, a semicircle of moderate diameter appears (curve 2), indicating some impedance to interface electron transfer. After incubation with the target protein, the impedance greatly increases (curve 3), manifesting as a fairly large semicircle, and this may represent proteins captured from the serum sample. After rinsing with a detergent, the semicircle decreases by a rather large portion (curve 4); this may be due to the fact that some proteins on the surface are interfering species adsorbed on the slide. However, the proposed method is to use the nonspecific proteins to amplify the signal, namely, directly cross-linking the target protein with the surrounding interfering proteins. Therefore, before rinsing the slide, it is placed under the illumination of visible light for proper time. Then, after detergent rinsing, the EIS spectrum is examined again (curve 5), and a dramatic increase of impedance can be observed. Since this is after detergent rinsing, it is relatively safe to infer that the increased impedance at step 5 is from the interfering proteins covalently cross-linked to the slide surface.

Subsequently, the time course of target–peptide interaction is further studied using EIS. As shown in Figure 3b, a control probe without the covalent "warhead" is first employed to target the main protease, and it takes nearly an hour for the noncovalent molecular recognition to reach equilibrium. However, after replacing the control peptide with the proposed probe, the time course is evidently shortened (Figure 3c, inset); around 10 min is enough for the covalent recognition to complete. This is because, although, as shown in Figure 1, the noncovalent recognition is much faster than the forming of a covalent bond; the noncovalent complex is also rather unstable. Therefore, the noncovalent interaction between the control probe and the target is actually a process of fast on and off reactions. As a result, for the target proteins noncovalently captured on the slide surface to withstand electrochemical

https://doi.org/10.1021/acssensors.1c00869
ACS Sens. 2021, 6, 2465–2471

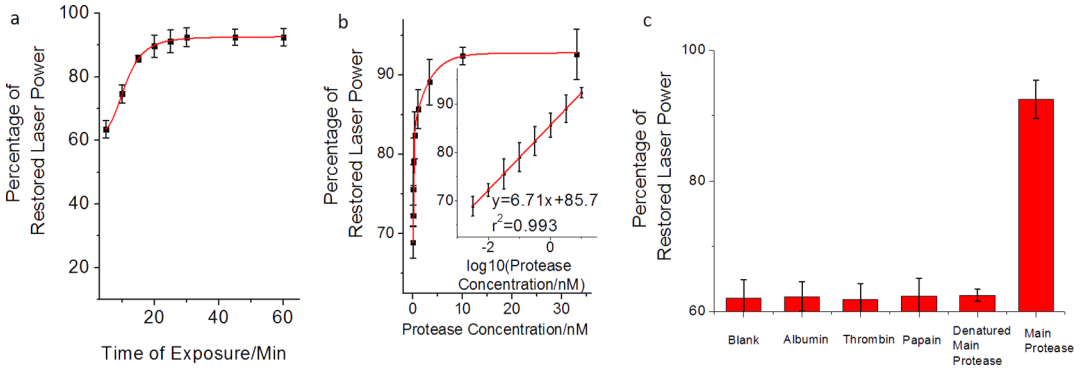

Figure 5. Readout of the laser power meter collected under various experimental conditions: (a) percentage of the restored laser power recorded in detecting 10 nM protease after incubating the stripped section of the fiber-optic cable with the serum-spiked sample, kept for a gradually longer time under visible-light illumination (detergent rinsing is conducted after light exposure). (b) Quantitative results recorded in detecting protease samples serially diluted using serum, the percentage of power restoration is plotted as a function of protease concentration, and error bars are the same as in the above figures. (c) Percentage of power restoration recorded in detecting the target protease and various control targets.

scanning and to yield the observed EIS signal, it takes a rather long period of time of incubation before the electrochemical measurements can be applied to the slide in order to reach a more stable equilibrium.

The next condition needed to be optimized is the time of exposure under visible-light illumination for the purpose of cross-linking with the interfering proteins in the clinical sample. It is to be noted that the cross-linking reaction takes place at the same time as the surface tethered probe molecules interact and covalently bind with the target protein. To find the proper time of incubation and exposure, it is first necessary to examine which of the two processes, namely, probe−target incubation and cross-linking with the interfering proteins, takes a longer time to complete. The time course of covalent bonding with the target protein has been found to approach completion after roughly 10 min (Figure 3c), while the time course of cross-linking is followed using the dityrosine fluorescent signal of the cross-linked product (Figure 4a). It takes more than 1 h for the fluorescent signal to reach a plateau, which means all the interfering proteins in the sample can be cross-linked at this time point. Therefore, it is now clear that the cross-linking of at least the large part of all interfering proteins in the clinical serum sample takes a much longer time to complete than the covalent targeting process.

Therefore, after incubating the slide with the serum sample, the incubation step can be just terminated after the covalent targeting process is completed in 10 min. However, cross-linking with the surrounding interfering species can directly influence the quality of the final signal readout. Figure 4b−d shows the fluorescent signals recorded for detecting the main protease of three different concentrations; each panel shows the response recorded at a specific time point during the process of exposure to visible-light radiation. It is evident that after 10 min of incubation to finish the covalent targeting process, a longer time of light exposure always produces a larger difference in the absolute fluorescent signal responses at the three protein concentrations.

However, a longer time of light exposure might not always be beneficial to the final signal readout of the proposed method: the above SPR, electrochemical, and fluorescent methods are all for characterizing the proposed biosensing mechanism. While the final signal readout is laser light, as mentioned ahead, after exposure to visible light, cross-linking of the serum sample produces a hydrogel cladding the stripped section of an optic fiber cable; without this layer of cladding, a large portion of the laser light will leak outside of the exposed silica core of the cable, so only residual laser light can continue flowing through the cable. This can be termed "mismatch" between the stripped section and the subsequent walled section of the cable. After the formation of the cladding gel around the stripped section, the "coupling" of the stripped and the subsequent walled section is restored, and the "mismatch" is overcome. Following this train of reasoning, more extensive cross-linking of the serum sample can result in more efficient "coupling" and more effective suppression of "mismatch". However, the reality is a little more complicated: excessive cross-linking in the hydrogel can result in the generation of the so-called evanescent waves, dissipating the light flow and reducing the final readout. Therefore, an optimal time of exposure must exist, under which condition the maximum laser readout can be achieved. As shown in Figure 5a, the optimal time of exposure is around 30 min.

Under the optimized conditions, quantitative detection can be achieved in detecting the recombinant SARS-Cov-2 main protease serially diluted with clinical serum samples collected from a healthy volunteer. As shown in Figure 5b, a quantitative working curve can be established between the percentage of laser power "coupling" and concentration of target protease. A limit of detection as low as 1 pM can be achieved, with a relatively large dynamic range from 3.3 pM to 10 nM. Figure 5c shows the specificity of detection, and it is clear that control targets cannot produce a nonnegligible signal response. Serum levels of this and other proteases have recently been correlated to the excessive immuno response leading to pulmonary failure and other lethal conditions after viral invasion.

CONCLUSIONS

We have developed a method requiring only a set of hand-held devices to achieve the quantitative detection of the main protease of SARS-Cov-2; no expensive antibodies, enzymes, and nanomaterials are needed; and only a sequence of simple and short peptide is enough to irreversibly target and bind with the protease. The method of signal readout is simple and straightforward: a section of wall has first been stripped off a piece of optic fiber cable and then cross-linking of the serum sample results in re-cladding of that stripped section, so that the leakage through this section can be restored. The covalent bonding between the probes and the target protease forms

https://doi.org/10.1021/acssensors.1c00869
ACS Sens. 2021, 6, 2465−2471

many "foothold" points, anchoring the cross-linking product to the silica core. In this manner, even after thorough rinsing, the cross-linking product can still be retained on the stripped cable. This method is successfully applied to detect the serum-spiked main protease of SARS-Cov-2, producing quantitative results.

AUTHOR INFORMATION

Corresponding Authors

Jialei Du − *Collaborative Innovation Center of Technology and Equipment for Biological Diagnosis and Therapy in Universities of Shandong, Institute for Advanced Interdisciplinary Research, University of Jinan, Jinan 250022, Shandong Province, P. R. China*; Email: ifc_dujl@ujn.edu.cn

Hao Li − *School of Biological Science and Technology, University of Jinan, Jinan 250022, Shandong Province, P. R. China*; orcid.org/0000-0001-7161-8949; Email: 2766300864@qq.com

Zhongyin Zhang − *Department of Medicinal Chemistry, School of Pharmacy, Qingdao University, Qingdao 266071, Shandong Province, China*; Email: zyzhang@qdu.edu.cn

Authors

Junxia Wang − *Department of Medicinal Chemistry, School of Pharmacy, Qingdao University, Qingdao 266071, Shandong Province, China*

Mengqi Lv − *Department of Medicinal Chemistry, School of Pharmacy, Qingdao University, Qingdao 266071, Shandong Province, China*

Hehuan Xia − *Collaborative Innovation Center of Technology and Equipment for Biological Diagnosis and Therapy in Universities of Shandong, Institute for Advanced Interdisciplinary Research, University of Jinan, Jinan 250022, Shandong Province, P. R. China*

Yiwei Zhao − *Collaborative Innovation Center of Technology and Equipment for Biological Diagnosis and Therapy in Universities of Shandong, Institute for Advanced Interdisciplinary Research, University of Jinan, Jinan 250022, Shandong Province, P. R. China*

Complete contact information is available at: https://pubs.acs.org/10.1021/acssensors.1c00869

Notes

The authors declare no competing financial interest.

ACKNOWLEDGMENTS

We acknowledge financial support of this work from the National Natural Science Foundation of China (22007053 to Z.Z. and 52002146 to J.D.) and the NSF of Shandong Province (ZR2018BH044 to Z.Z. and 2019GSF109013 and ZR2018BB035 to J.D.).

REFERENCES

(1) Fisher, J.; Languilaire, J.-C.; Lawthom, R.; Nieuwenhuis, R.; Petts, R. J.; Runswick-Cole, K.; Yerkes, M. A. Community, work, and family in times of COVID-19. *Community Work Fam.* **2020**, *23*, 247−252.

(2) Martin, A.; Markhvida, M.; Hallegatte, S.; Walsh, B. Socio-Economic Impacts of COVID-19 on Household Consumption and Poverty. *Econ. Disasters Clim. Change* **2020**, *4*, 453−479.

(3) Baggett, T. P.; Keyes, H.; Sporn, N.; Gaeta, J. M. Prevalence of SARS-CoV-2 Infection in Residents of a Large Homeless Shelter in Boston. *JAMA* **2020**, *323*, 2191−2192.

(4) Adhikari, S.; Pantaleo, N. P.; Feldman, J. M.; Ogedegbe, O.; Thorpe, L.; Troxel, A. B. Assessment of Community-Level Disparities in Coronavirus Disease 2019 (COVID-19) Infections and Deaths in Large US Metropolitan Areas. *JAMA Netw. Open* **2020**, *3*, No. e2016938.

(5) Trier, N.; Hansen, P.; Houen, G. Peptides, Antibodies, Peptide Antibodies and More. *Int. J. Mol. Sci.* **2019**, *20*, 6289−6311.

(6) Chen, K.; Zhou, J.; Shao, Z.; Liu, J.; Song, J.; Wang, R.; Li, J.; Tan, W. Aptamers as Versatile Molecular Tools for Antibody Production Monitoring and Quality Control. *J. Am. Chem. Soc.* **2020**, *142*, 12079−12086.

(7) Hasegawa, H.; Savory, N.; Abe, K.; Ikebukuro, K. Methods for Improving Aptamer Binding Affinity. *Molecules* **2016**, *21*, 421.

(8) Kimoto, M.; Shermane Lim, Y. W.; Hirao, I. Molecular affinity rulers: systematic evaluation of DNA aptamers for their applicabilities in ELISA. *Nucleic Acids Res.* **2019**, *47*, 8362−8374.

(9) Li, H.; Wang, F.; Ge, S.; Liu, H.; Yan, M.; Yu, J. Turning Nonspecific Interference into Signal Amplification: Covalent Biosensing Nanoassembly Enabled by Metal-Catalyzed Cross-Coupling. *Anal. Chem.* **2017**, *89*, 6834−6839.

(10) Li, H.; Huang, Y.; Yu, Y.; Wang, Y.; Li, G. Recognition-induced covalent capturing and labeling as a general strategy for protein detection. *Biosens. Bioelectron.* **2016**, *80*, 560−565.

(11) Buff, M.; Drab, E.; Sugihara, K. Effect of the nonspecific binding in differential impedance biosensing. *Biointerphases* **2019**, *14*, 011004.

(12) Zhang, L.; Lin, D.; Sun, X.; Curth, U.; Drosten, C.; Sauerhering, L.; Becker, S.; Rox, K.; Hilgenfeld, R. Crystal structure of SARS-CoV-2 main protease provides a basis for design of improved α-ketoamide inhibitors. *Science* **2020**, *368*, 409−412.

(13) Ullrich, S.; Nitsche, C. The SARS-CoV-2 main protease as drug target. *Bioorg. Med. Chem. Lett.* **2020**, *30*, 127377.

(14) Rut, W.; Lv, Z.; Zmudzinski, M.; Patchett, S.; Nayak, D.; Snipas, S. J.; El Oualid, F.; Huang, T. T.; Bekes, M.; Drag, M.; Olsen, S. K., Activity profiling and structures of inhibitor-bound SARS-CoV-2-PLpro protease provides a framework for anti-COVID-19 drug design. **2020**, bioRxiv:068890.

(15) Gao, T.; Xing, S.; Xu, M.; Fu, P.; Yao, J.; Zhang, X.; Zhao, Y.; Zhao, C. A peptide nucleic acid-regulated fluorescence resonance energy transfer DNA assay based on the use of carbon dots and gold nanoparticles. *Microchim. Acta* **2020**, *187*, 375.

(16) Alston, R. W.; Lasagna, M.; Grimsley, G. R.; Scholtz, J. M.; Reinhart, G. D.; Pace, C. N. Peptide sequence and conformation strongly influence tryptophan fluorescence. *Biophys. J.* **2008**, *94*, 2280−2287.

(17) Choi, J.-Y.; Lee, D.-I.; Kim, C.-J.; Lee, C.-H.; Ahn, I.-S. Synthesis of PEG hydrogel with dityrosine for multi-functionality and pH-dependent fluorescence. *J. Ind. Eng. Chem.* **2012**, *18*, 611−616.

(18) Lee, J.; Ju, M.; Cho, O. H.; Kim, Y.; Nam, K. T. Tyrosine-Rich Peptides as a Platform for Assembly and Material Synthesis. *Adv. Sci.* **2019**, *6*, 1801255.

(19) Fancy, D. A.; Kodadek, T. Chemistry for the analysis of protein-protein interactions: Rapid and efficient cross-linking triggered by long wavelength light. *Proc. Natl. Acad. Sci. U.S.A.* **1999**, *96*, 6020−6024.

(20) Mendes, S. B.; Saavedra, S. On probing molecular monolayers: a spectroscopic optical waveguide approach of ultra-sensitivity. *Opt. Express* **1999**, *4*, 449−456.

(21) Martínez-Fleta, P.; Alfranca, A.; González-Álvaro, I.; Casasnovas, J. M.; Fernández-Soto, D.; Esteso, G.; Cáceres-Martell, Y.; Gardeta, S.; López-Sanz, C.; Prat, S.; Mateu-Albero, T.; Gabrie, L.; López-Granados, E.; Sánchez-Madrid, F.; Reyburn, H. T.; Rodríguez Frade, J. M.; Valés-Gómez, M. SARS-CoV-2 Cysteine-like Protease Antibodies Can Be Detected in Serum and Saliva of COVID-19-Seropositive Individuals. *J. Immunol.* **2020**, *205*, 3130−3140.